Communicated by Sidney Lehky

# Directional Filling-in

**Karl Frederick Arrington**
*Department of Brain and Cognitive Sciences,*
*Massachusetts Institute of Technology, Cambridge, MA 02139 USA*

**The filling-in theory of brightness perception has gained much attention recently owing to the success of vision models. However, the theory and its instantiations have suffered from incorrectly dealing with transitive brightness relations. This paper describes an advance in the filling-in theory that overcomes the problem. The advance is incorporated into the BCS/FCS neural network model, which allows it, for the first time, to account for all of Arend's test stimuli for assessing brightness perception models. The theory also suggests a new teleology for parallel ON- and OFF-channels.**

## 1 Introduction

Light intensity reflected from a surface changes dramatically with change in illumination, but the ratio of intensities (contrast) reflected from adjacent locations remains essentially constant. The visual system extracts the contrast ratio from the distribution of light hitting the retina by local differencing mechanisms of two types: *on-center/off-surround* detectors that respond maximally to a light spot surrounded by a dark annulus, and *off-center/on-surround* detectors that respond maximally to a dark spot surrounded by a lighter annulus. These two distinct populations appear at retinal ganglion cells that project to the visual cortex.

Given that the information sent from the retina to the brain is primarily about local luminance and color contrasts rather than about extended areas, why do we experience object surfaces, rather than mere edges? One explanation is that information from the edges "flows" across the areas that correspond to uniform surfaces, filling them in with features such as color and brightness. Numerous examples of filling-in phenomena appear in the clinical literature: from retinal scotomas (Gerrits and Timmerman 1969), and from experimental work using stabilized images (Krauskopf 1963; Gerrits *et al.* 1966; Yarbus 1967). There is also a growing literature on the filling-in of texture information from human psychophysics (Ramachandran and Gregory 1991; Ramachandran *et al.* 1992) and from single unit recording (De Weerd *et al.* 1993).

 

## 2 Models

Gerrits and Vendrik (1970) developed a qualitative model of the filling-in phenomenon by specifying a *filling-in process* that works in parallel with a *filling-in barrier* mechanism. According to their filling-in theory, the ON- and the OFF-responses, which peak on opposite sides of a contour edge, fill in over areas that correspond to uniform regions of the stimulus. Mixing of the antagonistic activities is prevented by a boundary, or barrier, that is created at the locations where contrast is high (edges). Grossberg and his colleagues (Grossberg 1983; Cohen and Grossberg 1984; Grossberg and Todorović 1988) have mathematically specified a neural network model of filling-in called the *boundary contour system/feature contour system* (BCS/FCS) model that instantiates the filling-in theory of Gerrits and Vendrik (1970). The BCS and FCS systems work in parallel: the FCS discounts variable illumination and the BCS generates an emergent boundary segmentation of a scene. The signals from these two systems interact to create visible percepts by filling in surface features within segmentation boundaries. Studies of the temporal dynamics of the BCS/FCS model under visual masking conditions (Arrington 1994a) strongly support the Stoper and Mansfield (1978) conjecture that *area-suppression* masking is mediated by a sluggish high level filling-in system that follows the fast low-level system mediating *contour-suppression* masking.

Arend (1983) presented a set of test stimuli for assessing brightness perception models. Though the BCS/FCS model has proven successful in predicting the brightness percepts of a variety of stimulus distributions, its ability to account for Arend's complete set has never been demonstrated. This failure occurs because the theory and the model have never dealt adequately with transitive luminance stimuli, in other words, stimuli that have successive contrasts in the same direction: for example, a staircase of luminance steps, as in Figure 1.

This paper describes an advance to the filling-in theory, called *directional filling-in* (DFI). According to DFI, local contrasts build upon the foundation of surrounding brightness levels, rather than being isolated by surrounding boundary signals. The DFI theory is implemented by modifying the BCS/FCS model to include a *directional filling-in gate* (DFIG) that is explained later. Model performance is evaluated using a variety of stimuli. For each stimulus, the brightness predictions from the Grossberg and Todorović (1988) version of the BCS/FCS model (henceforth referred to as the GT88 model) and from the BCS/FCS with directional filling-in gates (henceforth referred to as the DFIG model) are compared. The GT88 model was chosen for comparison because it is arguably the best known example of traditional filling-in theory and because it has served as a common starting point for a number of derivative models (for example, see Neumann (1993) that is discussed later). It will be shown that the DFIG model accounts for all stimuli in Arend's set for evaluat-

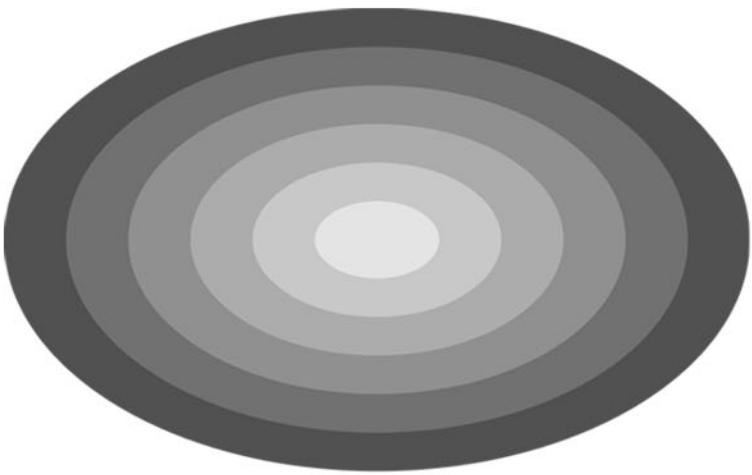

Figure 1: Illustration of transitive luminance steps. This pyramid stimulus illustrates the type of successive increments (or decrements) in luminance that have been problematic for filling-in theory.

ing brightness models, including those with transitive relations—such as multiple cusps and steps, and cusp-separated pedestals—for which the GT88 model does not account, while retaining the ability to account for the Tolhurst effect (Tolhurst 1972).

## 3 The Theory of the Directional Filling-in

A schematic comparison of the traditional Gerrits–Vendrik–Cohen–Grossberg filling-in theory to the DFI theory is shown in Figure 2. Notice that the FCS response depends only on local stimulus contrasts. Consequently, brightness predictions, which are manifest as filled-in activities, depend only on the brightness (darkness) signals contained within a region that is partitioned by the associated boundary. This brightness prediction scheme effectively isolates the input contrast responses in one part of the visual field from those in another part of the field, forming "watertight," noninteracting compartments. Successive luminance steps will tend to appear the same brightness because each isolated brightness and darkness response is identical (see Fig. 2).

To overcome the isolation, DFI specifies that each local brightness step builds upon the foundation of previous brightness levels. In a comple-

mentary fashion, the darkness also builds upon itself in the activation levels of the OFF-channel filling-in layer. This is accomplished by injecting the lower brightness (darkness) levels up into areas of greater brightness (darkness). Figure 2b illustrates how these signals build upon one another in parallel in the ON- and OFF-filling-in layers.

One possible neural implementation of the DFI theory is illustrated in Figure 3. In this model, the upward flow is instantiated by lateral synaptic connections that are facilitated by simple-cells sensitive to the appropriate direction of contrast. Figure 3 (top) shows a luminance stimulus contrast; just below are the FCS ON- and OFF-responses to local contrast. Next are the simple cells' responses to oriented contrasts. Opposite direction-of-contrast simple cells with the same orientation are added to create a complex cell response that is the BCS boundary to filling-in. In the GT88 model (and presumably in the Gerrits and Vendrik theory, though this is never specified), the boundaries to filling-in are insensitive to direction-of-contrast information, whereas in DFI, the direction-of-contrast information is retained and utilized. Cells $S_i$ are filling-in layer cells, whose lateral connections allow diffusive filling-in of feature information. This diffusive filling-in is restricted by boundary-modulated gates, $G$. Given the stimulus pattern at the top of the figure, a high resistance gate signal (black vertical bar) would form between filling-in layer cells $S_i$ and $S_{i+1}$. Since the stimulus is a step up to the right, the directional gates, $U$ (indicated by white terminal buttons), are active, which facilitates ON-channel activation of cell $S_{i+1}$ by cell $S_i$ via the rightward directed axon projection (white arrow), and OFF-channel activation of cell $S_i$ by cell $S_{i+1}$ via the leftward directed axon projection (black arrow). This type of system can function properly only if both ON- and OFF-responses operate in the same manner, and suggests an important new role for this parallel system, which is discussed further in Section 5.1.

The DFIG mechanism complements the diffusion mechanism that is restricted at the boundaries. It is of interest just how beneficial the addition of this *local* DFIG mechanism can be to generating accurate *global* brightness predictions.

## 4 Comparison of Model Equations

First the GT88 model is fully explained, then the DFIG augmentation is elaborated. Both neural network models consist of a series of feedforward layers beginning with an input layer, $I_{ij}$, where the luminance stimuli are presented, and followed by a series of neural processing layers. The last neural layer, $O_{ij}$, is the output of the model, which shows the predicted brightness perception. The activation of the neurons is determined by differential equations, as described below. The models do not differ substantially in the FCS layer (Section 4.1) or the BCS layer

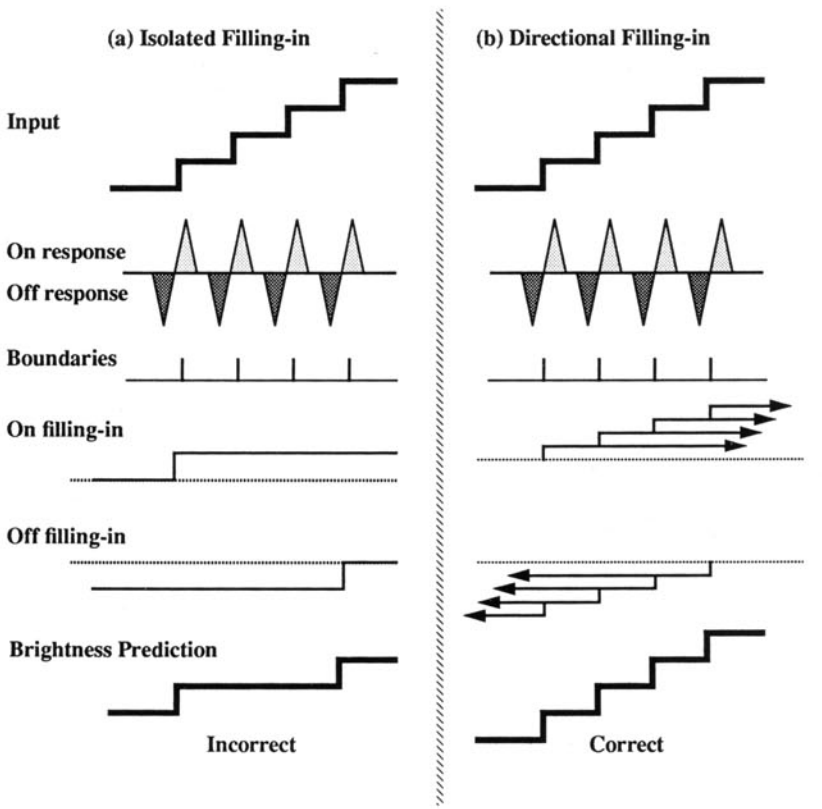


Figure 2: Schematic comparison of traditional filling-in theory (a) to directional filling-in (DFI) theory (b) using transitive luminance steps. The input (top row) is the same to both models, as are the ON- and OFF-responses and the boundary responses. The main difference appears at the filling-in stage. In the traditional theory, contrast information is partitioned by the boundary signals so equal ON- and OFF-signals will *cancel* to produce a net eigengrau brightness percept. In the DFI theory, activity is injected across boundary partitions in the direction of increase. That is, where brightness increases, brightness signals are injected across boundaries to form a brightness floor in the next region, against which the next brightness signal can deflect. In a complementary fashion, successive darkness signals build upon one another. The result is that DFI produces a more accurate brightness prediction.

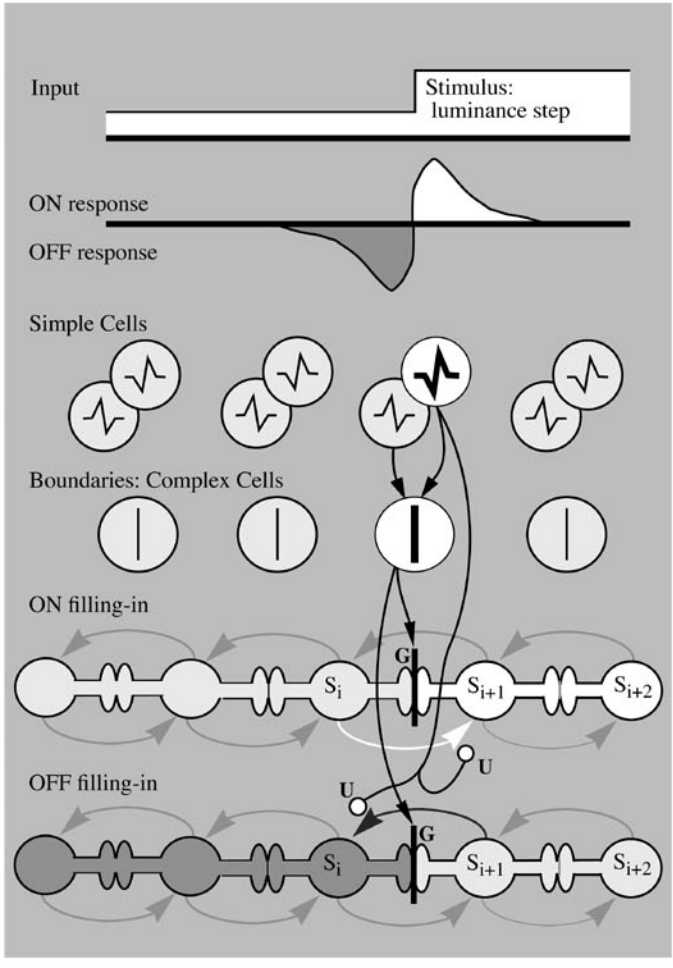


Figure 3: A physiologically plausible neural model using directional filling-in gates. Cells $S_i$ are filling-in layer cells; lateral connections allow diffusive filling-in of feature information. This diffusive filling-in is restricted by boundary-modulated gates, $G$. Given the stimulus pattern at the top of the figure, a high resistance gate signal would form between filling-in layer cells $S_i$ and $S_{i+1}$. Since the stimulus is a step up to the right, the directional filling-in gates, $U$ (indicated by white terminal button), allow brightness activation to flow rightward in the ON-fil!ing-in layer and darkness activation to flow leftward in the OFF-filling-in layer.

(Section 4.2); compare Figure 2a and Figure 2b. As far as possible, the DFIG equations have been kept identical to those for the GT88 model. The important difference between the GT88 model and the DFIG model appears at the filling-in layer (Sections 4.3 and 4.4).

**4.1 Feature Contour System.** The FCS specifies how a light stimulus to the eye is sampled by ON- and OFF-channel retinal ganglion cells through a center/surround receptive field anatomy. The network equations used to model the retinal ganglion cells, $x_{ij}^{(c)}$, are shown in equations 4.1 and 4.2. The superscript, (c), indicates the *channel*, that is, whether it is an ON-center cell or an OFF-center cell. Parameters $P_x$, $D_x$, and $H_x$ are the passive decay rate, depolarization limit, and hyperpolarization limit of the neuron, respectively. For the *on-center/off-surround* cells the variables $I_{ij}^{(\text{center})}$ and $I_{ij}^{(\text{surround})}$ are the total excitatory and total inhibitory inputs to the neuron, respectively, such that

$$\frac{dx_{ij}^{(\text{ON})}}{dt} = -P_x x_{ij}^{(\text{ON})} + (D_x - x_{ij}^{(\text{ON})})I_{ij}^{(\text{center})} - (x_{ij}^{(\text{ON})} + H_x)I_{ij}^{(\text{surround})} \quad (4.1)$$

These are reversed for the *off-center/on-surround* cell

$$\begin{aligned}\frac{dx_{ij}^{(\text{OFF})}}{dt} &= -P_x x_{ij}^{(\text{OFF})} + (D_x - x_{ij}^{(\text{OFF})})I_{ij}^{(\text{surround})} \\ &\quad - (x_{ij}^{(\text{OFF})} + H_x)I_{ij}^{(\text{center})}\end{aligned} \quad (4.2)$$

These total inputs are specified as

$$I_{ij}^{(\omega)} = W_\omega \sum_{p,q} \Psi_{pqij}^{(\omega)} I_{pq} \quad (4.3)$$

where $W_\omega$ is the weighting coefficient and

$$\Psi_{pqij}^{(\text{w})} = \exp\{-\lambda_{\text{w}}^{-2}(\log[2])[(p-i)^2 + (q-j)^2]\} \quad (4.4)$$

is the gaussian distribution that specifies the center and surround receptive fields, which compose the difference of gaussians (DOG) receptive field. Parameter $\lambda_\omega$ in equation 4.4 specifies the spatial bandwidth of the gaussian receptive field.

The equilibrium response of equation 4.1 is

$$x_{ij}^{(\text{ON})} = \frac{\sum_{p,q}(DW_{\text{r}}\Psi_{pqij}^{(\text{r})} - HW_{\text{s}}\Psi_{pqij}^{(\text{s})})I_{pq}}{P_x + \sum_{p,q}(W_{\text{r}}\Psi_{pqij}^{(\text{r})} - W_{\text{s}}\Psi_{pqij}^{(\text{s})})I_{pq}} \quad (4.5)$$

where $r$ indicates center and $s$ indicates surround.

The FCS output is the half-wave rectified cell potential

$$X_{ij}^{(\text{ON})} = \max(x_{ij}^{(\text{ON})}, 0) \quad (4.6)$$

That is, the cell fires at a rate proportional to the depolarization level, but is silent when the cell is hyperpolarized.

**4.2 The Boundary Contour System.** The BCS generates an emergent boundary segmentation of the scene. First cortical *simple cells* detect colinear contrasts, then *complex cells* combine the same orientation, but opposite direction-of-contrasts responses from the simple cells. At each spatial location, activations from complex cells of all orientations are combined to form a *total boundary signal* that is passed through a *compressive nonlinear* (sigmoid) transfer function to produce the final boundary signal.

The first stage of the boundary system, equation 4.7, specifies a model "simple cell" that responds to oriented activations across the field of $X_{ij}$. The activities $y_{ijk}$ of the oriented contrast-sensitive cells centered at location $(i, j)$ with orientation $k$, obey the additive equation

$$\frac{dy_{ijk}}{dt} = -y_{ijk} + \sum_{p,q} X_{pq}^{(\mathrm{ON})} \Phi_{pqij}^{(k)} \tag{4.7}$$

Equation 4.8 specifies the oriented receptive field, $\Phi_{pqij}^{(k)}$, of orientation $k$, which is created using a difference-of-offset-gaussians (DOOG), as follows. The gaussian kernel that forms the negative part of the oriented contrast detector is spatially offset from the location of the detecting cell by vector $(-m_k, -n_k)$,

$$\Phi_{pqij}^{(k)} = \phi_{p,q,i,j} - \phi_{p,q,(i-m_k),(j-n_k)} \tag{4.8}$$

where

$$\phi_{pqij} = \exp\{-\gamma^{-2}[(p-i)^2 + (q-j)^2]\} \tag{4.9}$$

and where

$$m_k = \sin\frac{2\pi k}{K} \tag{4.10}$$

and

$$n_k = \cos\frac{2\pi k}{K} \tag{4.11}$$

where $K$ is the total number of differently oriented contrasts.

The potentials from the set of orientation sensitive cells, $y_{ij}$, are half wave rectified to obtain

$$Y_{ijk} = \max(y_{ijk}, 0) \tag{4.12}$$

The rectified potentials of the two "simple cells" with the same orientation, but with opposite directions of contrast, are linearly combined to form a "complex cell," $b_{ijk}$, that is sensitive to orientation, but insensitive to direction of contrast,

$$b_{ijk} = Y_{ijk} + Y_{ij[k+(K/2)]} \tag{4.13}$$

The output from these cells is threshold rectified,

$$B_{ijk} = \max(b_{ijk} - L, 0) \tag{4.14}$$

where parameter $L$ specifies how much contrast is required before a boundary signal is created. A total BCS signal, $B_{ij}$ (without subscript $k$), is created by summing the response of all the oriented boundary signals, $B_{ijk}$ (with subscript $k$), at location $(i, j)$

$$B_{ij} = \sum_k B_{ijk} \tag{4.15}$$

The final BCS signal is insensitive not only to direction of contrast, but also to contrast orientation.

In some simulations published in Grossberg and Todorović (1988) the boundary signal was transformed

$$\mathbf{B}_{ijk} = s(B_{ijk}) \tag{4.16}$$

through the compressive nonlinearity

$$s(x) = k_1 x^{\vartheta} / (k_2 + x^{\vartheta}) \tag{4.17}$$

(Grossberg and Todorović 1988, pp. 262, 277). This type of transfer function is used to render the boundary signal more uniform in size and to more effectively reduce the diffusion between boundary compartments. All GT88 simulations here use $\mathbf{B}_{ijk}$ to extend the useful contrast range.

**4.3 The GT88 Model Filling-in Process.** Finally, the FCS and BCS provide parallel input to the filling-in layer. The ON- and OFF-activations flow into each other and cancel except where flow is impeded by high resistance boundary signals. The FCS signals, $X_{ij}^{(\mathrm{ON})}$ and $X_{ij}^{(\mathrm{OFF})}$, which are active only at locations immediately adjacent to stimulus contrasts, are fed into the filling-in layer where the activity freely spreads across neighbor cells. This diffusive filling-in process is impeded by high resistance gating signals, $G_{pqij}$, between locations $(i, j)$ and $(p, q)$ that are activated by BCS boundaries. The equation for the filling-in layer potential, $S_{ij}$, is

$$\frac{dS_{ij}^{(\mathrm{c})}}{dt} = -P_{\mathrm{S}} S_{ij}^{(\mathrm{c})} + X_{ij}^{(\mathrm{c})} + F_{ij}^{(\mathrm{c})} \tag{4.18}$$

where $P_{\mathrm{S}}$ is the passive decay rate constant, the $X_{ij}^{(\mathrm{c})}$ term is the *direct input* from the FCS, and the $F_{ij}^{(\mathrm{c})}$ term is the *lateral diffusion* (filling-in) term

$$F_{ij}^{(\mathrm{c})} = \sum_{(p,q)\in N_{ij}} [(S_{pq}^{(\mathrm{c})} - S_{ij}^{(\mathrm{c})}) G_{pqij}] \tag{4.19}$$

The term $(S_{pq} - S_{ij})$ in equation 4.19 is a discrete approximation to the Laplacian diffusion operator, since the set $N_{ij}$ of locations comprises only

the lattice of nearest neighbors of $(i,j)$

$$N_{ij} = \{(i,j-1),(i-1,j),(i+1,j),(i,j+1)\} \tag{4.20}$$

The diffusion gating coefficients, $G_{pqij}$, that regulate the lateral spread of activation are the same for each channel (c) and depend on the spatially adjacent BCS signals, $B_{ij}$ and $B_{pq}$, as follows:

$$G_{pqij} = \frac{\delta}{1+\varepsilon(B_{pq}+B_{ij})} \tag{4.21}$$

Parameter $\delta$ controls the rate of diffusion. A large value will allow rapid diffusion from the edges across uniform areas, which results in a smoother appearance. A smaller value will cause input activation to accumulate where it is input near the boundaries. Parameter $\varepsilon$ controls the diffusion across boundaries. A large value allows little diffusion across boundaries.

The GT88 model used only $X_{ij}^{(\mathrm{ON})}$. By making the excitatory center more heavily weighted than the surround (i.e., unbalanced), the $x_{ij}^{(\mathrm{ON})}$ contained a large positive dc response, i.e., the response to uniform areas was well above zero. Consequently, there was little rectification (equation 4.6) of the hyperpolarization associated with the dark side of a contrast. This allowed the hyperpolarizations to be used in the stead of OFF-responses. As long as the input contrasts are not too large, this corresponds adequately and avoids computing parallel ON- and OFF-signals in subsequent stages, as well as avoids the need to recombine them. For conformity to previously published work, as well as for fair comparison of models, the GT88 simulations use the original model. The DFIG model performs better with a balanced DOG; nevertheless, by the same argument, the DFIG simulations use

$$X_{ij}^{(\mathrm{OFF})} = \max(-x_{ij}^{(\mathrm{ON})}, 0) \tag{4.22}$$

Grossberg (1987b) makes it clear that the BCS/FCS theory calls for parallel ON- and OFF-filling-in channels. In general, the brightness percept output of the model, $O_{ij}$, is assumed to be additive such that

$$O_{ij} = S_{ij}^{(\mathrm{ON})} - S_{ij}^{(\mathrm{OFF})} \tag{4.23}$$

Nevertheless, the GT88 model simulations used only $S^{(\mathrm{ON})}$. As will be seen next, the DFIG model requires that the ON- and OFF-filling-in channels be calculated separately.

**4.4 Directional Filling-in Gate Equations.** The DFIG model is theoretically equivalent to the GT88 model, except for the addition of the directional filling term, $J_{ij}^{(c)}$, in the filling-in equation, which now becomes

$$\frac{d\hat{S}_{ij}^{(c)}}{dt} = -P_S\hat{S}_{ij}^{(c)} + X_{ij}^{(c)} + F_{ij}^{(c)} + J_{ij}^{(c)} \tag{4.24}$$

where

$$J_{ij}^{(c)} = \sum_{(p,q)\in N_{ij}} [\hat{S}_{pq}^{(c)} \times U_{pqij}^{(c)}] \tag{4.25}$$

The directional gate $U_{pqij}^{(c)}$, used in term $J_{ij}^{(c)}$, depends on the channel (c), whereas the gate $G_{pqij}$, used in term $F_{ij}^{(c)}$ (see equation 4.19), does not. The directional gate that allows activation to flow upward to areas of increasing brightness or increasing darkness is modeled as

$$U_{pqij}^{(c)} = g(X_{ij}^{(c)} - X_{pq}^{(c)} - \theta_{UX})h(B_{pq}B_{ij} - \theta_{UB}) \tag{4.26}$$

To fix ideas, equation 4.26 says: activate directional flow where there exists a sufficient boundary, $h(B_{ij}B_{pq} - \theta_{UB})$, and where the feature signal shows an *increase* of activation (brightness or darkness), $g(X_{ij}^{(c)} - X_{pq}^{(c)} - \theta_{UX})$. The directional filling-in term, $S_{pq}U_{pqij}^{(c)}$, injects activation proportional to the lower side, $S_{pq}$, according to some function of the feature signal magnitude, $U_{pqij}^{(c)}$. Note that in the case where $g(x)$ is always zero, equation 4.24 reduces to equation 4.18. In the simulations presented here, the simplest directional function is chosen

$$g(x) = \begin{cases} k_t \leftarrow \text{If } (x > 0) \\ 0 \leftarrow \text{otherwise} \end{cases} \tag{4.27}$$

and the boundary function, $h$, is the unit step function at zero.

The boundary gates and the directional gates are complementary. Where there is no border present, $G_{pqij}$ is significant and large, which allows passive diffusion through term $F_{ij}$, but $U_{pqij}$ is insignificant; on the other hand, where a border is present, the directional gate, $U_{pqij}$, is significant and allows flow through term $J_{ij}$, but $G_{pqij}$ is insignificant and resistance is high.

**4.5 Simulation Methods.** The DFIG simulations presented here are designed to evaluate the DFI theory and to build intuition about it. To facilitate these goals, the simulations employ an ideal implementation of the DFIG projection field that is a single filling-in cell wide. (In general this would not be the case, as is elaborated in the discussion.) Consequently, the simulations require very sharp and precise boundary signals. Specifically, the additive difference-of-offset-gaussians (DOOG) equation in the DFIG simulations is

$$\hat{b}_i = \left(\sum_p X_p^{(\mathrm{ON})} \Upsilon_{pi}\right) \left(\sum_p X_p^{(\mathrm{OFF})} \Upsilon_{pi}\right) \tag{4.28}$$

where each kernel, $\Upsilon$, is $\{1, 1, 1\}$. This signal is then thresholded

$$\hat{B}_{ijk} = \max(\hat{b}_{ijk} - L, 0) \tag{4.29}$$

as in equation 4.14 and transformed as in equation 4.16, to become

$$\hat{\mathbf{B}}_{ijk} = s(\hat{B}_{ijk}) \tag{4.30}$$

A sharper diffusion gate, $\hat{G}$, between two filling-in cells is obtained by multiplying, rather than adding, the adjacent boundary cells, such that

$$\hat{G}_{pqij} = \frac{\delta}{1 + B_{pq}B_{ij}} \tag{4.31}$$

The expanded one-dimensional DFIG equation is

$$\frac{d}{dt}\hat{S}_i^{(c)} = -P_S\hat{S}_i^{(c)} + \sum_{p\in N}\left[(\hat{S}_p^{(c)} - \hat{S}_i^{(c)})\hat{G}_{pi} + \hat{S}_p^{(c)}U_{pi}^{(c)}\right] + X_i^{(c)} \tag{4.32}$$

The steady-state solutions can be found by solving the linear system

$$\overline{\overline{M}}\,\overline{S} = \overline{X} \tag{4.33}$$

where $M$ is a banded system matrix, which in the one-dimensional case is of the form

$$\begin{aligned}\overline{\overline{M}} \;=\; & -\hat{S}_{i-1}(\hat{G}_{i,i-1} + U_{i,i-1}) + \hat{S}_i(P_S + \hat{G}_{i,i-1} + \hat{G}_{i,i+1}) \\ & - \hat{S}_{i+1}(\hat{G}_{i,i+1} + U_{i,i+1})\end{aligned} \tag{4.34}$$

The DFIG kernels were numerically normalized (such that the sum of the kernel elements equals unity) then multiplied by 100. The remaining parameters in the equation were chosen such that spatially uniform stimuli yield a zero response, specifically $(DW_r - HW_s) = 0$. Normalization assures a completely balanced center and surround, which helps guarantee symmetric ON- and OFF-responses. In all simulations, these spatial bandwidths of the excitatory and inhibitory kernels of the receptive fields are the same in both the GT88 model and the DFIG model.

To help isolate and illustrate the key concept of the DFI theory, the filling-in layer diffusion parameter, $\delta$, was increased so as to produce more uniform brightness levels within bounded areas. This also helps reduce perceptual illusions from the line levels in the simulation results. All parameters are listed in the Appendix; they were the same in all simulations in this paper.

## 5 Comparison of Brightness Prediction

Brightness predictions of the GT88 model and of the DFIG model are compared using a variety of luminance stimuli. The one-dimensional stimuli should be understood as profiles cut through the two-dimensional brightness displays that historically have been created by rotating disks (Cornsweet 1970). Both the theory and the model can easily be extended to two dimensions.

**5.1 Parallel DFI Channels: The Pyramid.** The staircase pyramid luminance stimulus, shown in Figure 4a, is particularly useful in illustrating the behavior and the power of DFI. The luminance steps consist of equal ratio increments so the contrast for each step is the same and the FCS response to each step is identical, as shown in Figure 4b. The BCS signal is shown in Figure 4c. Traditional isolated filling-in occurs everywhere except at boundary locations, as indicated by diffusion gate activity shown in Figure 4d. The rightward and leftward DFIG activities for the ON-channel are shown in Figure 4e and Figure 4f, respectively; the OFF-channel DFIG activities are the same except that their locations correspond to locations of increasing darkness.

Notice the systematic compression in the ON- and OFF-filling-in layers, which occurs with a succession of steps in the same direction. Each brightness increase in the ON-channel, Figure 4g, is increasingly small (signal compression), but the same effect is occurring in the OFF-channel, Figure 4h, where each increase in darkness is successively smaller. When these two nonlinear channels are additively combined, the systematic biases tend to cancel! This suggests a new theoretical reason for the existence (teleology) of parallel ON- and OFF-channels. The result is a more accurate, linear brightness prediction by the DFIG-model, shown in Figure 4j. The GT88 model predicts only flat brightness steps, Figure 4i.

**5.2 A Battery of Test Stimuli.** Arend (1983) presents a set of luminance stimuli developed by O'Brien (1958) and Cornsweet as a test set for assessing brightness perception models. These stimuli are contained in Figure 5 together with the Tolhurst stimulus, Figure 5g, and a bull's eye stimulus, Figure 5l. The luminance stimuli and the associated human psychophysical brightness percepts are shown in the first two columns; the last two columns show the brightness predictions of the GT88 and DFIG models, respectively. Each of the Arend (1983) brightness predictions in the DFIG set and in the GT88 set was scaled as a group so the abscissa and ordinate values are the same for each.

The eight top rows, Figure 5a–h, show correct brightness predictions by both models. The last four rows, Figure 5i–l, show cases where only the DFIG model makes acceptable brightness predictions. Figure 5l shows a saw-tooth stimulus that produces a bull's eye brightness percept (Arend *et al.* 1971). Here, the gain of the GT88 brightness prediction has been amplified to illustrate an interesting brightness inversion that can occur in the center ring. This inversion was considered a success by Grossberg and Todorović, who argued that when using small patterns on large backgrounds, their informal psychophysical observations were in the same direction as the simulation results. However, Arend could not find such effects when he used larger stimuli.[1]

[1]See Grossberg and Todorović (1988) pp. 261–262 for a discussion of this.

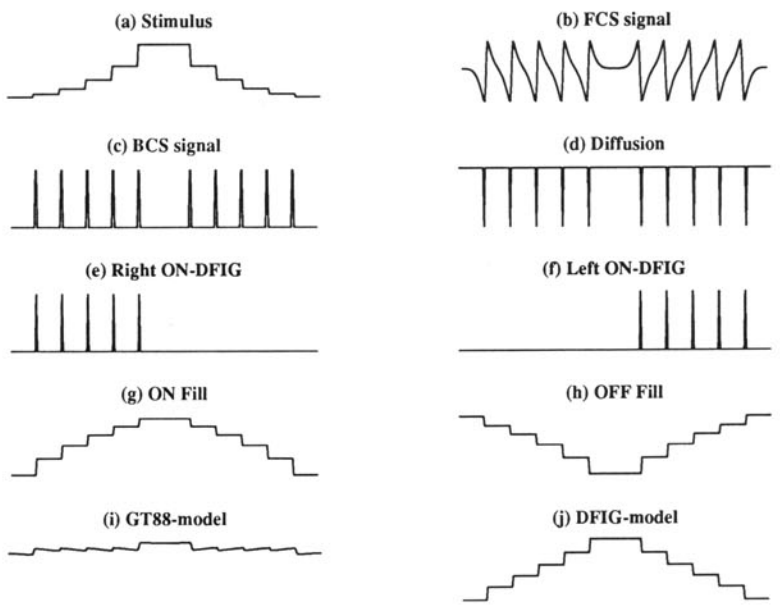


Figure 4: Experiment using staircase luminance stimulus (pyramid). The stimulus consists of equal ratio luminance increments. The rightward and leftward DFIG activities are shown for the ON-channel. Notice how the compressive nonlinear activations in the ON- and OFF-filling-in layers cancel to produce a linear brightness increase percept in the DFIG model.

## 6 Discussion

The results show that DFI provides accurate perceptual brightness predictions for a wide variety of luminance stimuli, particularly where transitive luminance distributions exist. Moreover, this is accomplished at a single spatial scale! The model requires, and thus provides rationale for, separate ON- and OFF-channels. Next, the distinction between the DFI theory and possible DFIG model implementations is elaborated. Finally, a comparison between DFI and alternative approaches to the problem of brightness prediction is discussed.

**6.1 Implementation Issues.** This study was designed to test the theory of DFI. To facilitate a focused study of the DFIG behavior across transitive luminance distributions, the current implementation used DFIG receptive and projective fields limited to a single cell directly adjacent

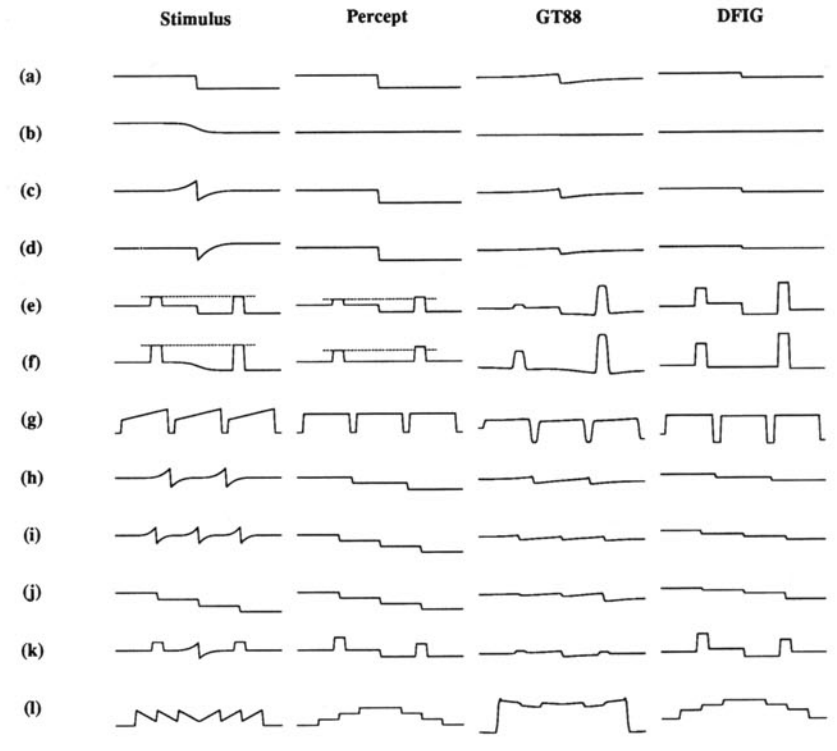


Figure 5: A battery of test stimuli. Various luminance stimuli and the associated human psychophysical brightness percepts are shown in the first two columns. The last two columns show the brightness predictions of the GT88 model and the DFIG model, respectively. The DFIG model performs well for all stimuli, whereas the GT88 model performs well only for (a) through (h).

to the boundary. In general, the DFIG projection field should coincide with the spatial scale of the FCS, which would allow thick boundaries and slower diffusion to be reinstated, which in turn would allow the DFI model to count the Mach Band effects and the Chevreul illusion effects as successes just as the GT88 model did.

The DFI theory is not wedded to the particular mechanism described here. The DFIG is only one of a number of local mechanisms that can affect global brightness perception. One alternative mechanism could employ facilitation of the FCS cells that project to the filling-in layer, such that the gain of the FCS signal is proportional to the activation of

the adjacent filling-in region. By using the same FCS projection field, the DFI and FCS spatial scales are guaranteed to be the same.

**6.2 Comparison with Alternative Approaches.** Previous attempts to deal with the transitivity problem have involved symbolic rule based systems such as MIRAGE (Watt and Morgan 1985) and MIDAAS (Kingdom and Moulden 1992). The DFIG model can in some ways be considered a neural implementation of the symbolic brightness rule for steps.

There are several other possible solutions to the problem of transitivity. One solution may be to combine contrast information obtained at multiple spatial scales. It is clear that multiple spatial channels operate in parallel in the visual system (Wilson *et al.* 1990) and they have been qualitatively discussed by Grossberg (1987a). When Arend made a critique of an early version of the BCS/FCS (Grossberg 1983) because of its inability to handle all of the cases in the test set, Grossberg used a multiple spatial scale justification as a rejoinder; however, simulations have yet to appear. It should be noted that the Kingdom and Moulden (1992) model used multiple spatial scales, but symbolic brightness step rules were still required to handle the transitive cases.

Another solution may be to allow some direct-intensity information, as well as the contrast-intensity information. Some researchers believe that the retinal ganglion cells may transmit at least a little direct-intensity information in addition to the contrast-intensity information that most strongly affects them. This type of absolute intensity information has been used in resistive grid models to solve a related problem—namely, because the Land (1986) algorithm operates under a *gray world assumption*: one obtains grayness from large uniform fields (e.g., the sky) and sudden appearance of color when objects appear (e.g., a few birds fly over). Within the framework of the retinex model, Moore and colleagues have employed a homomorphic-filter transfer function that is itself a function of local "edginess" in the stimulus, so that contrast information is used when it is available; otherwise direct information is used (Moore *et al.* 1991a,b).

Direct intensity information has been incorporated into a variant of the BCS/FCS developed by Neumann (1993), who points out that the shunting equations (equations 4.1 and 4.2) allow for a scaled low-pass filter encoding of stimulus luminance distributions, as well as providing saturation levels for the DOG contrast response. Neumann argues that the ON- and OFF-pair provide multiplexed contrast (polarity) and luminance information. His model has demonstrated some successes with actual luminance steps; however, it does not appear that this or any direct intensity model can ever account for the brightness illusions such as the brightness staircase perception from multiple cusps. It is still far from certain that sufficient direct intensity information is actually transmitted to the brain, and retinal stabilization experiments argue against its significance.

## 7 Conclusion

It has been demonstrated that the directional filling-in (DFI) extension to traditional filling-in theory provides more accurate predictions of perceptual brightness from a variety of luminance stimuli, particularly with the class of stimuli that has successive luminance steps or cusps in the same direction. The entire set of brightness experiments described by Arend *et al.* (1971) for assessing brightness models is simulated here for the first time using the BCS/FCS model with the DFIG augmentation; moreover, it is accomplished within a single spatial scale. Finally, the DFI theory provides a new teleology for the parallel ON- and OFF-channels. DFI is of course not limited to brightness perception—it should apply equally well to any feature that is perceived to fill in, including color, depth, and texture.

## 8 Appendix: Parameters

The parameters in parentheses refer to the equations in Grossberg and Todorović (1988). The GT88 parameters used in all simulations shown in this paper are

(A) $P_x = 1$; (B) $D_x = 90$; (C) $C = 4$; (D) $H_x = 60$; (E) $E = 0.5$;

(L) $L = 5$; $(\alpha)\lambda_{(\text{center})} = 1$; $(\beta)\ \lambda_{(\text{surround})} = 8$; (M) $P_S = 10$; $\delta = 100{,}000$; $\varepsilon = 100$; $\gamma = 1$; $k_1 = 10$; $k_2 = 1$; $\vartheta = 5$.

The DFIG parameters used in all simulations shown in this paper are

(A) $P_x = 0.1$; (B) $D_x = 2.5$; (C) $C = 1.0$; (D) $H_x = 1.0$; (E) $E = 2.5$;

(L) $L = 0.001$; $(\alpha)\ \lambda_{(\text{center})} = 1$; $(\beta)\ \lambda_{(\text{surround})} = 8$; (M) $P_S = 1$; $\delta = 500{,}000$; $\varepsilon = 500{,}000$;

$\gamma = 1$; $k_1 = 1$; $k_2 = 0.0001$; $\vartheta = 1$; $k_t = 10$; $\theta_{UX} = 0.0$; $\theta_{UB} = 0.02$.

In Figure 5, the width of the input layer and the neural fields were all 150 processing units (cells), except for Figure 5l that used a width of 118. The stimulus in Figure 5l was constructed to illustrate an interesting brightness inversion that can occur in the GT88 model in certain input parameter ranges. Since the brightness percepts in Figure 5i and 5j are the same and represent half of a rotating disk, the percept for Figure 5l was obtained by flipping one and concatenating it to the other.

## Acknowledgments

I would like to thank Stephen Grossberg, Michael Cohen, Ennio Mingolla, and Richard Held for their support and encouragement. The work described in this paper was supported by a grant from the Office of Naval

Research, ONR N00014-91-J-4100, while in the Cognitive and Neural Systems Department Ph.D. program at Boston University (Arrington 1993), and through a fellowship from the McDonnell-Pew Center for Cognitive Neuroscience at MIT (Arrington 1994b).

## References

Arend, L. 1983. "Filling-in" between edges. *Behav. Brain Sci.* **6**, 657–658.

Arend, L., Buehler, J. N., and Lockhead, G. R. 1971. Difference information in brightness perception. *Percept. Psychophys.* **9**(3B), 367–370.

Arrington, K. F. 1993. Neural network model of color and brightness perception and binocular rivalry. Unpublished Ph.D. Thesis, Cognitive and Neural Systems Department, Boston University, Boston, MA.

Arrington, K. F. 1994a. The temporal dynamics of brightness filling-in. *Vision Res.* **34**(24), 3371–3387.

Arrington, K. F. 1994b. Visual feature-flow using directional ionic-gates. *ARVO Abstr. Invest. Ophthalmol. Visual Sci.* **35**(4, suppl.), 2005.

Cohen, M. A., and Grossberg, S. 1984. Neural Dynamics of brightness perception: Features, boundaries, diffusion, and resonance. *Percept. Psychophys.* **36**(5), 428–456.

Cornsweet, T. N. 1970. *Visual Perception.* Harcourt Brace Jovanovich, New York.

De Weerd, P., Gattas, R., Desimone, R., and Ungerleider, L. G. 1993. Center-surround interactions in areas V2/V3: A possible mechanism for filling-in? *Neurosci. Abstr.* **19**.

Gerrits, H. J. M., and Timmerman, G. J. M. E. N. 1969. The filling-in process in patients with retinal scotomata. *Vision Res.* **9**, 439–442.

Gerrits, H. J. M., and Vendrik, A. J. H. 1970. Simultaneous contrast, filling-in process and information processing in man's visual system. *Exp. Brain Res.* **11**, 411–430.

Gerrits, H. J. M., de Haan, B., and Vendrik, A. J. H. 1966. Experiments with retinal stabilized images. Relations between the observations and neural data. *Vision Res.* **6**, 427–440.

Grossberg, S. 1983. The quantized geometry of visual space: The coherent computation of depth, form, and lightness. *Behav. Brain Sci.* **6**, 625–692.

Grossberg, S. 1987a. Cortical dynamics of three-dimensional form, color and brightness perception: I. Monocular theory. *Perception Psychophysics* **41**(2), 87–116. Pagination references are to the reprinted version in Grossberg, S. (ed.) 1988. *Neural Networks and Natural Intelligence*, Chap. 1, pp. 1–54. MIT Press, Cambridge, MA.

Grossberg, S. 1987b. Cortical dynamics of three-dimensional form, color and brightness perception: II. Binocular theory. *Percept. Psychophys.* **41**(2), 117–158. Pagination references are to the reprinted version in Grossberg, S. (ed.). 1988. *Neural Networks and Natural Intelligence*, Chap. 2, pp. 55–126. MIT Press, Cambridge, MA.

Grossberg, S., and Todorović, D. 1988. Neural dynamics of 1-D and 2-D bright-

ness perception: A unified model of classical and recent phenomena. *Percept. Psychophys.* **43**, 241–277.

Kingdom, F., and Moulden, B. 1992. A multi-channel approach to brightness coding. *Vision Res.* **32**(8), 1565–1582.

Krauskopf, J. 1963. Effect of retinal image stabilization on the appearance of heterochromatic targets. *J. Opt. Soc. Am.* **53**(6), 741–744.

Land, E. H. 1986. Recent advances in retinex theory. *Vision Res.* **26**(1), 7–21.

Moore, A., Allman, J., and Goodman, R. M. 1991a. A real-time neural system for color constancy. *IEEE Trans. Neural Networks* **2**(2), 237–247.

Moore, A., Fox, G., Allman, J., and Goodman, R. 1991b. A VLSI neural network for color constancy. In *Advances in Neural Information Processing Systems 3*, D. S. Touretzky and R. Lippman, eds., IEEE Conference Proceedings, Nov. 26–29, 1990. Morgan Kauffman, San Mateo, CA.

Neumann, H. 1993. Toward a computational architecture for unified visual contrast and brightness perception: I. Theory and model. *Proc. World Congress Neural Networks (WCNN'93)* July 11–15, (I) 84–91.

O'Brien, V. 1958. Contour perception, illusion and reality. *J. Opt. Soc. Am.* **48**, 112–119 (re-referenced).

Ramachandran, V. S., and Gregory, R. L. 1991. Perceptual filling in of artificially induced scotomas in human vision. *Nature (London)* **350**, 699–702.

Ramachandran, V. S., Gregory, R. L., and Aiken, W. 1992. Perceptual fading of visual texture border. *Vision Res.* **33**(5/6), 717–721.

Stoper, A. E., and Mansfield, J. G. 1978. Metacontrast and paracontrast suppression of a contourless area. *Vision Res.* **18**, 1669–1674.

Tolhurst, D. J. 1972. On the possible existence of edge detector neurons in the human visual system. *Vision Res.* **12**, 797–804.

Watt, R. J., and Morgan, M. J. 1985. A theory of the primitive spatial code in human vision. *Vision Res.* **25**(11), 1661–1674.

Wilson, H. R., Levi, D., Maffei, L., Rovamo, J., and DeValois, R. 1990. The perception of form. In *Visual Perception: The Neurophysiological Foundations*, L. Spillmann and J. S. Werner, eds., Chap. 10, pp. 231–272. Academic Press, New York.

Yarbus, A. L. 1967. *Eye Movements and Vision*. Plenum Press: New York.

Received November 18, 1994; accepted July 18, 1995.